LUNFD-6-NFFL-7069-1992
RETAIN
Fermilab Library
0 1160 0015573 3

LUNFD 6/(NFFL-7069) 1992

Asymmetries in Jet Azimuthal Angle Distributions as a Test of QCD*

V. Hedberg[a], G. Ingelman[b], C. Jacobsson[a], L. Jönsson[a]

[a] Dept. of Elementary Particle Physics, Lund University, Lund, Sweden
[b] DESY, Hamburg and Dept. of Radiation Sciences, Uppsala University, Sweden

Abstract: First order QCD matrix elements predict a specific dependence in azimuthal angle (around the DIS current direction) of the produced jets which, at HERA energies, gives a new test of QCD. We show how the QCD Compton process can be used for this purpose, taking experimental effects into account. In the analysis we introduce a novelty in the jet finding procedure and we separate quark and gluon jets by using a neural network.

MAY 1 1992
FERMILAB

1 Introduction

The description of the hadronic final state in deep inelastic scattering (DIS) is influenced by perturbative QCD in several ways, as can be calculated through exact matrix elements or leading log parton showers [1]. In this study we will consider the distribution of jets in azimuthal angle Φ around the exchanged boson direction since this has been proposed as a suitable test for first order QCD matrix elements [2]. However, at low energies the expected effect is masked by the influence of the primordial transverse momentum [3, 4] and the hadronization, which are described by non-perturbative QCD. Thus, the effect from the underlying perturbative parton process has not been possible to observe in lepton scattering experiments on fixed targets [5]. With increasing energy, the perturbative effect is expected to dominate over the non-perturbative ones and the situation should therefore be more favourable at HERA energies [6]. In the following we will investigate the prospects for such a QCD test at HERA. To be realistic, we have performed a full event simulation and have taken experimental effects into account by using a detector simulation program.

2 The QCD Φ-dependence

The hadronic final state is best studied in its own center-of-mass system (cms), i.e. the cms of the exchanged boson and the proton. A z-axis along the proton direction can then be chosen to define longitudinal and transverse momentum components. The angle we consider is the azimuthal angle around this axis and with $\Phi = 0$ defined by the scattered lepton, which together with the incoming one forms the lepton scattering plane shown in Fig. 1. In the naive quark-parton model (QPM) the incoming quark will be back-scattered along this z-axis. However, in first order QCD processes such as QCD Compton

*Submitted to the Proceedings of the HERA Workshop 1992

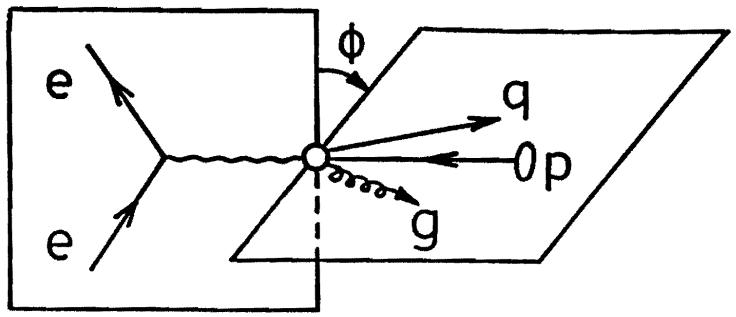

Figure 1: *The first order QCD Compton process, $\gamma^* q \rightarrow qg$, viewed in the hadronic (i.e. boson-proton) center-of-mass system. The lepton scattering plane and the parton plane are shown as well as the azimuthal angle around the boson direction with $\Phi = 0$ defined by the scattered lepton.*

($\gamma^* q \rightarrow qg$) and boson-gluon fusion (BGF) ($\gamma^* g \rightarrow q\bar{q}$) two final partons will emerge with some transverse momenta. These transverse momenta will balance (neglecting primordial $k_\perp$ to be discussed below) and therefore define the 'parton plane' as illustrated in Fig. 1. The azimuthal angle between this plane and the lepton scattering plane has a non-trivial distribution given by the QCD matrix elements [2, 6] that can be schematically written

$$\frac{d\sigma}{dcos\Phi} = A + B\, cos\Phi + C\, cos2\Phi \tag{1}$$

where A, B and C are given by QCD. The complete first order cross-section is five-fold differential and depends, in addition to Φ, on the normal DIS kinematic variables x and Q^2 as well as on two extra variables needed to specify energy and polar angle of one parton (the other parton follows by energy-momentum conservation). Thus, A, B and C will in general depend on these variables (except Φ) or the integral over some of them if a more inclusive cross-section is considered. In particular, B and C tend to increase with $p_\perp$ of the partons.

In the case of the incoming quark having a non-zero primordial transverse momentum $k_\perp$, reflecting the Fermi motion in the proton, it will be back-scattered keeping its transverse momentum such that an azimuthal angle can also be defined in the zero-order QPM process. The resulting Φ-distribution is not flat, but leads to an asymmetry that is different from the one in the first order QCD process [3, 4]. In addition, the fluctuations in hadronization, which are essentially symmetric around the quark momentum direction, will tend to reduce the Φ-asymmetries at the hadron level. Both these non-perturbative transverse momentum effects should be limited to a few hundred MeV and, therefore, play less of a role in events with large $p_\perp$ which are dominated by the QCD process. At the relatively low cms energies in fixed target scattering experiments, however, the cross-section at sufficiently high $p_\perp$ is too small and the previous analyses [5] have been dominated by the Φ-dependence due to the non-perturbative effects and, in fact, have been used to estimate $k_\perp$.

The following study is based on the simulation of complete events using the AROMA [7] and LEPTO [8] Monte Carlo programs, based on the exact, fully differential first order

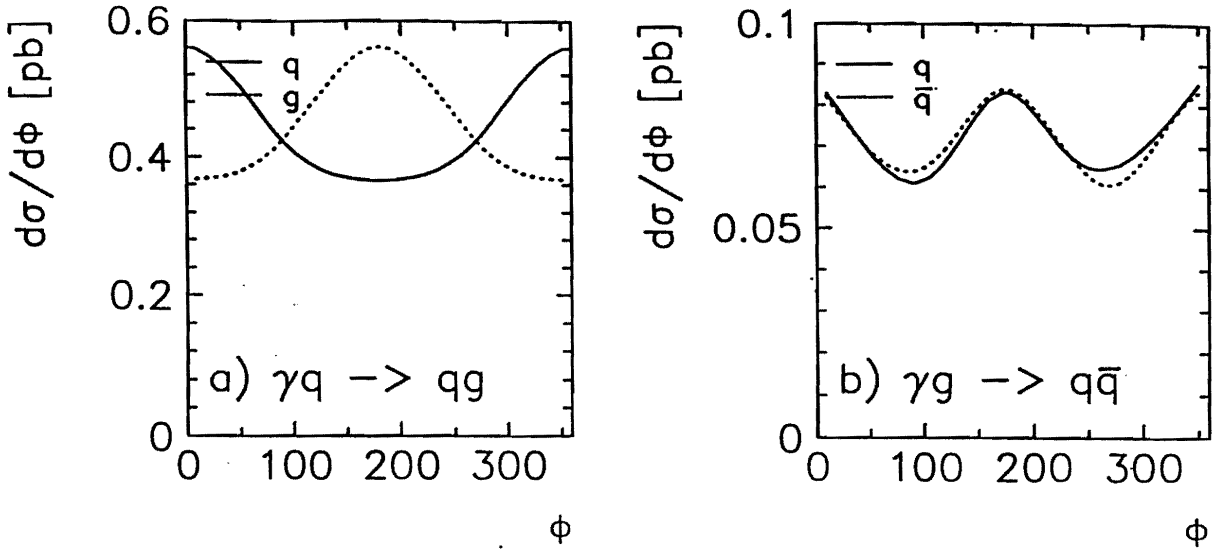

Figure 2: *Differential cross-section versus azimuthal angle for partons, with $p_\perp \geq 4$ GeV, produced by (a) the QCD Compton and (b) the boson-gluon fusion processes, (in the selected kinematic region shown in Fig. 4).*

QCD matrix elements. Primordial transverse momentum is included using the conventional Gaussian distribution (with a width of 440 MeV) and hadronization is performed using the Lund model [9, 10].

The Φ-dependence of partons with $p_\perp \geq 4$ GeV is shown in Fig. 2 for both the QCD Compton and the boson-gluon fusion processes. These distributions are different and tend to give a reduced effect if added. Therefore it is preferable to separate the two processes to make the interpretation clearer. In this sense one process is the background to the other. In the QCD Compton case, the quark and the gluon have opposite distributions that would cancel the effect if added. The proper way to resolve this is, of course, to separate the two by identification of quark and gluon jets. It may also be possible to add them with their energies as weights relying on the fact that the quark jet usually is more energetic in this frame. In the fusion process there is symmetry between the quark and the antiquark such that their distributions can simply be added. As an overall measure of these Φ-asymmetries one can use

$$\langle cos\Phi \rangle = \frac{B}{2A}, \quad \langle cos2\Phi \rangle = \frac{C}{2A} \tag{2}$$

which thus directly measure the QCD coefficients, since A can be obtained from the jet rate integrated over Φ. The parton level distributions of these quantities are shown in Fig. 3, which demonstrate the increasing asymmetry with increasing parton $p_\perp$. In the Compton case, the asymmetry increases strongly up to about 4 GeV after which it tends to level off. In the subsequent analysis we require the jet to have $p_{\perp jet} \geq 4$ GeV to obtain a significant asymmetry and to ensure a suitable region for perturbative QCD. From Fig. 2 and 3 it is clear that the Compton process will have a significant contribution from the $cos\Phi$ term but only a small one from the $cos2\Phi$ term, whereas the situation is quite the opposite for the fusion process.

The size of the effect also depends on the event kinematics and, in particular, the asymmetry is larger for larger x. In the following analysis, we have concentrated on the QCD Compton process and return in the concluding discussion to the BGF process. The

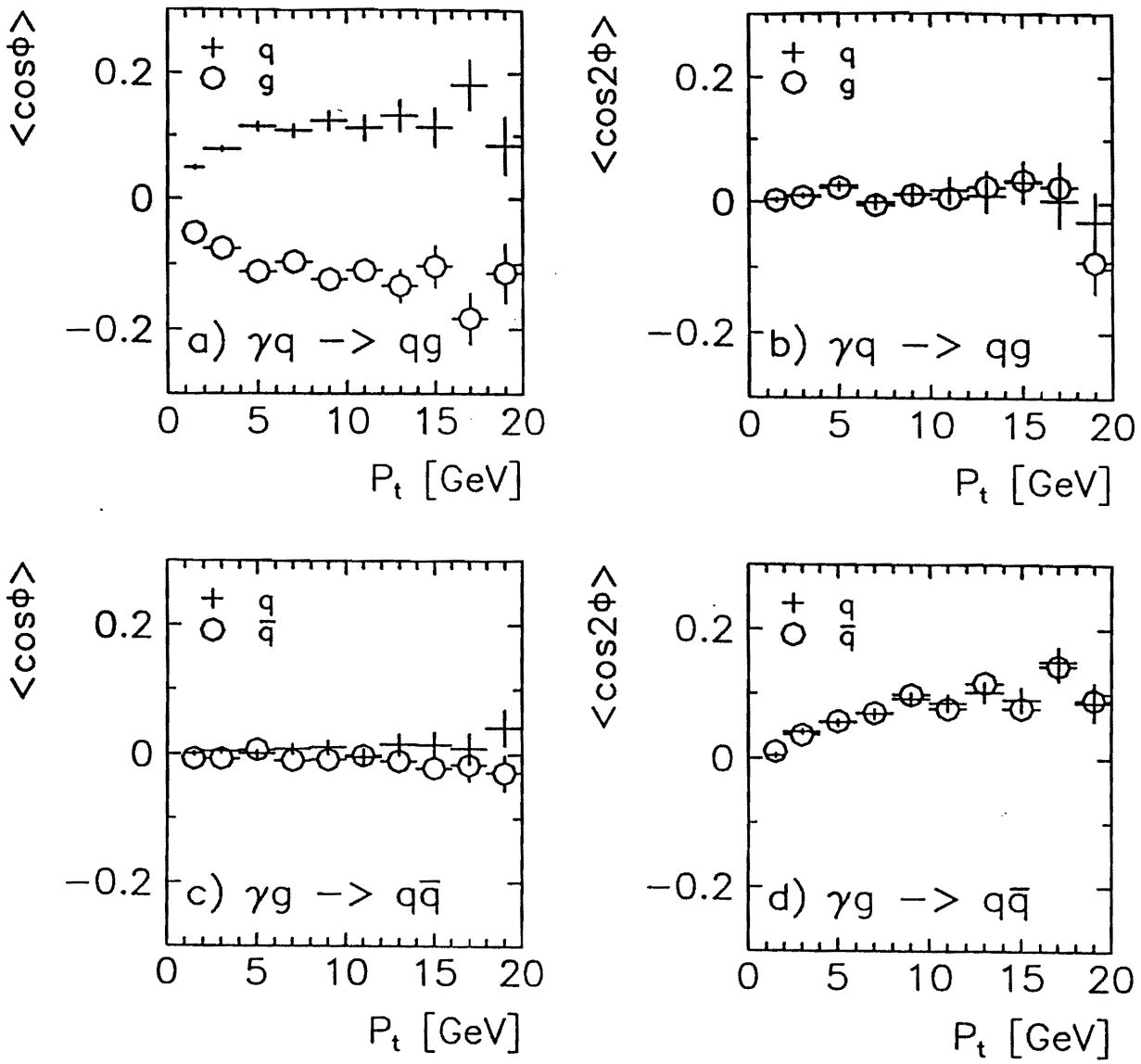

Figure 3: *Azimuthal asymmetries of the partons produced in (a,b) the QCD Compton process and (c,d) the boson-gluon fusion process versus the parton transverse momentum. The kinematic region of Fig. 4 is selected and the error bars correspond to an integrated luminosity of 100 pb^{-1} illustrating an ideal (parton level) measurement.*

choice of the kinematic region shown in Fig. 4 is based on several criteria that must be fulfilled. The lower limit in y is motivated by the measurement of the scattered electron, which is needed to define $\Phi = 0$ as well as to reconstruct x and Q^2 for the transformation to the hadronic cms. The relatively large x-values enhance both the size of the azimuthal asymmetry and improves the ratio of the signal (QCD Compton) to the BGF 'background' which has a softer x-distribution governed by the gluon distribution. The ratio of cross-sections in this region is, for $p_\perp \geq 4$ GeV,

$$\frac{\sigma(\gamma q \to qg)}{\sigma(\gamma g \to q\bar{q})} = \frac{160\ pb}{46\ pb} = 3.5 \tag{3}$$

giving a favourable signal-to-background ratio, which may be further improved by either applying some event topology cuts or exploiting the quark/gluon jet separation discussed below. This dominant background, as well as others, are therefore neglected in the following. To perform this QCD test one must thus measure the scattered electron, reconstruct

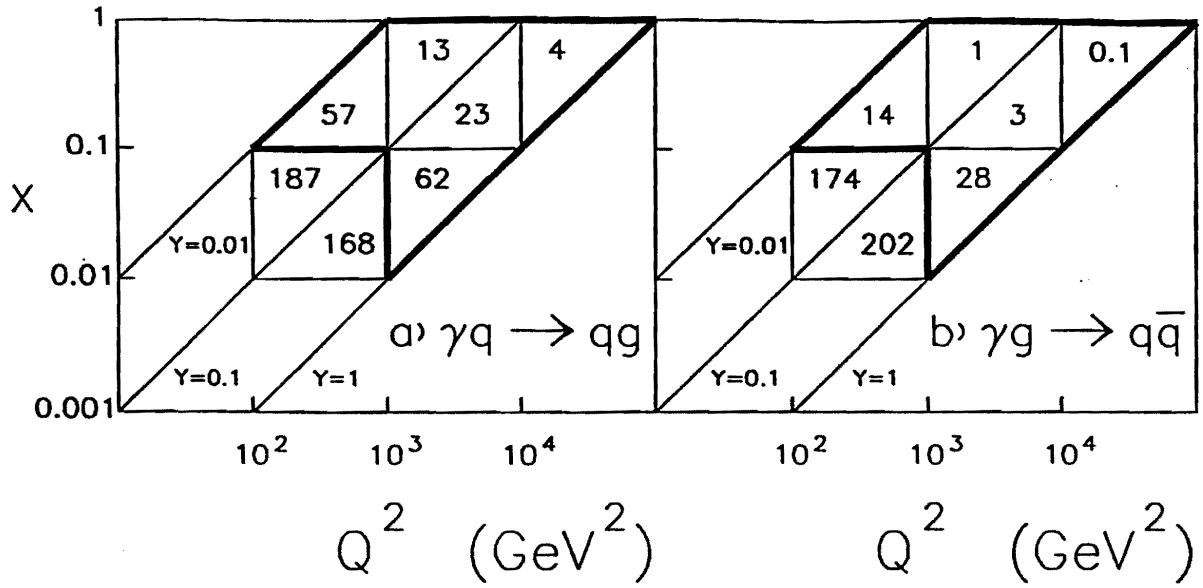

Figure 4: *The kinematic region marked by the thick black line was selected in this analysi Cross-sections in pb are given for (a) the QCD Compton signal process and (b) the fusion 'background' process. The parton level cross-section for $p_\perp \geq 4$ GeV are shown.*

the event kinematics and select the above x, Q^2-region. Jets have to be found and identified as quark or gluon jets and their azimuthal distributions in the hadronic cms have to be measured and compared with the QCD expectations.

3 Experimental aspects

In order to investigate the influence of the H1-detector on the generated events, we applied the detector simulation program H1PSI [11] and for the analysis of the resulting detector output we used the tools provided by the physics analysis package H1PHAN [12]. Energy clusters in the calorimeters were formed by the program PACLUS [11], which was tuned to give somewhat fewer clusters than real particles.

3.1 Electron tagging and reconstruction of event kinematics

All particles that gave rise to a track, which was uniquely connected to a cluster with more than 90% of its energy in the electromagnetic part of the calorimeter, were classified as electrons and were hence candidates for being the scattered electron. In our kinematic region, the scattered electron has always an angle greater than 20° (relative to the incoming electron) and an energy larger than 10 GeV. Requiring our candidates to fulfill these criteria in addition, gave a reliable identification of the scattered electron such that in 90% of the events an electron fulfilling these requirements was found and the probability of missidentification was very low.

As mentioned, the kinematics of the event has to be determined to allow for a transformation into the hadronic center of mass system. We have compared the results from a reconstruction of the kinematic variables, when only the information from the scattered

electron was used, with the 'double angle' method [13], where information also from the hadronic system was included (in our case based on the calorimeter only). The double angle method is slightly better in our kinematic region and can be expected to deteriorate less when initial QED radiation is taken into account.

3.2 Jet reconstruction

For the jet reconstruction, we have only used the calorimeter information and not yet exploited the expected improvement, on the jet four-vector reconstruction, when including information from the tracking devices. Jets were found using the JADE algorithm in LUCLUS [10], where the pair of particles (or clusters) with the smallest invariant mass are joined into a cluster. The procedure is then repeated until all remaining pairs have an invariant mass exceeding a cut-off, i.e. $m_{ij}^2 > y_{cut}M^2$ where M is a suitable reference-mass such as the invariant mass W of the hadronic system. The final clusters then represent the jets in the event. Although most of the spectator-jet will escape down the beampipe, some of its fringe particles might still hit the detector. Since all particles are assigned to a jet, this may cause either extra jets or biases of other jets and it is therefore important to also reconstruct the spectator-jet properly. For this purpose, we introduced a 'pseudo-particle' with a momentum equal to the measured missing longitudinal momentum. This will ensure that the observed particles from the hadronization of the proton remnant will, to a large extent, be correctly associated with the spectator-jet.

We have found that using the hadronic mass W as a reference in the jet algorithm is not appropriate for our purposes (and most likely also not in other cases). In our kinematic region, W^2 can vary by several orders of magnitude ($W^2 = Q^2(1-x)/x + m_p^2$), whereas the squared invariant mass $\hat{s}$ of the quark-gluon system is rather constant around 200 GeV^2. The cut in the invariant mass squared, $m_{ij}^2 = y_{cut}W^2$, of a jet, will thus not scale according to the hard scattering process, as desired, but the quark and gluon jets will be treated differently in different kinematic regions.

To overcome this problem, we introduced a new feature in the jet reconstruction procedure by dividing it into two steps. First the jet algorithm was applied to the complete event, including the pseudo-particle, using W as the reference mass. This gave a good reconstruction of the spectator-jet since the mass-cut varies properly with its angular separation from the remaining hadronic system. This latter system, with mass W_{rem}, is then associated with the hard scattering system, i.e. the quark-gluon system with mass squared $\hat{s}$. The y_{cut}-parameter was tuned to give the optimal agreement between W_{rem}^2 and $\hat{s}$ and we show the result in Fig. 5a obtained for $y_{cut} = 0.06$. (The small bump at large positive values is due to cases where the gluon jet is not separated from the spectator-jet. Since this affects the reconstructed spectator-jet, it can be removed by a cut on the angle of the spectator-jet.) In the second step, the particles belonging to the spectator-jet was removed and the jet algorithm applied to the remaining system, but with W_{rem} as the proper reference scale for the hard scattering system. For our purposes we now tuned the y_{cut}-parameter to give the maximum number of two-jet events, however, still keeping it large enough to avoid creating artificial extra jets which could make normal one-jet DIS events look like QCD Compton events. Choosing $y_{cut} = 0.18$, we obtained the jet multiplicity shown in Fig. 5b for our kinematic region.

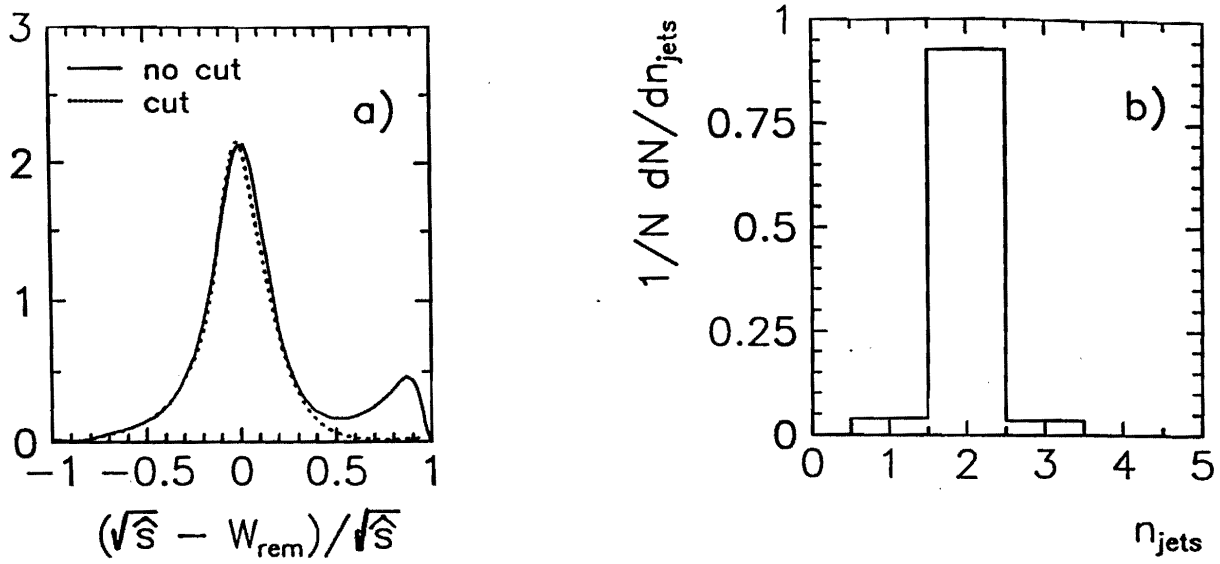

Figure 5: *(a) The relative error in the reconstructed invariant mass $\sqrt{\hat{s}}$ of the hard scattering quark-gluon system (with and without cut in the angle of the spectator-jet). (b) The jet multiplicity distribution for QCD Compton events after removing the spectator-jet and repeating the jet finding algorithm.*

3.3 Transformation to the hadronic cms

To make the transformation into the hadronic cms, where the azimuthal angle has been defined, we calculated the four-vector PH_i of the hadronic system in the following way:

$$\begin{aligned} PH_x &= -\cos\Phi_\ell E_\ell \sqrt{1-\cos^2\theta_\ell} \\ PH_y &= -\sin\Phi_\ell E_\ell \sqrt{1-\cos^2\theta_\ell} \\ PH_z &= E_p - E_e - E_\ell \cos\theta_\ell \\ PH_E &= E_p + E_e - E_\ell \end{aligned} \tag{4}$$

where x, y and Q^2 are obtained from the double angle method giving $E_\ell = E_e(1-y) + \frac{Q^2}{4E_e}$ whereas Φ_ℓ and θ_ℓ are determined directly from the measured electron. In particular the reconstruction of PH_x and PH_y was improved using the double angle method compared to when only the information from the scattered electron was used. PH_x and PH_y

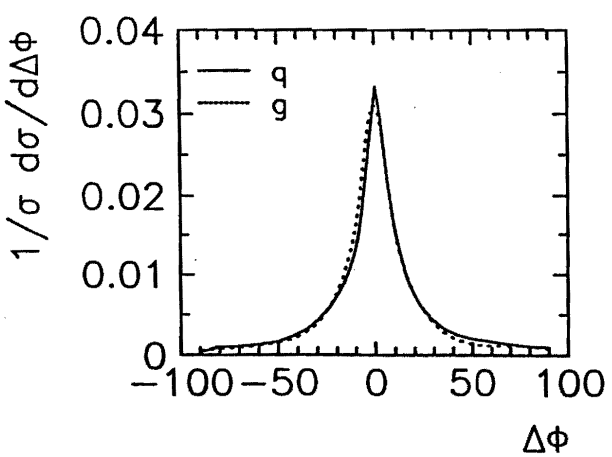

Figure 6: *The distribution of the error on the azimuthal angle (in degrees) of the reconstructed jets, taking detector simulation effects into account.*

are used in the transverse boost and, as can be understood from Fig. 1, the resulting azimuthal angle is affected by the transverse boost but not by the longitudinal one. After the transformation has been completed, rotations are performed to obtain the initial proton momentum along the z-direction and the transverse momentum components of the electrons along the x-direction. The resulting absolute error on the reconstructed azimuthal angles of the jets is shown in Fig. 6.

3.4 Jet identification using a neural network

As explained in section 2, the quark and gluon jet should preferably be identified to get an optimal result. Such an identification has to be based on characteristic differencies in the production and hadronization of these partons. This is a typical feature recognition problem well suited for a neural network.

A neural network [14] has a hierarchic structure of several layers of nodes (neurons) where each node is connected via synapses to every other node in the adjacent layers. The number of nodes should be correlated to the number of input parameters presented to the network. The latter number depends in turn on how many variables that are sensitive to differencies in the objects to be separated. The input data are given to the lowest layer of the network and are then fed through the synapses, where the input values are weighted, to the nodes in the next layer. A transfer function in each node converts the sum of all input values from the incoming synapses, to an output value that is passed on further up in the network. In the hidden layers, i.e. layers between the input and output layer, an internal representation of the observed data is constructed and in the top layer the data is put into different categories. The network has to go through a learning procedure in which a data sample (most often Monte Carlo generated) with known properties is used as input. The weighting at the synapses will then be adjusted to minimize the error in categorizing the data. The data sample is presented to the network repeatedly until this error is acceptably small.

We have used the program package JETNET 2.0 [15] to construct our network, a Multilayer Perceptron, and we have applied a 'backpropagation' learning procedure. The architecture of the network consisted of 10 input nodes, 15 hidden nodes and 1 output node. As input to the network we have selected the following quantities that show differences between quark and gluon jets (cf. Fig. 7ab):

- the energy of the jet, E_{jet}, and
- the nine most distinguishing Fodor moments: $F_{00}, F_{01}, F_{02}, F_{10}, F_{11}, F_{12}, F_{13}, F_{21}, F_{310}$.

The Fodor moments [16] are defined as $F_{mn}(E_{jet}) = \sum_i \left(\frac{p_{ti}}{E_{jet}}\right)^m \eta_i^n$ where the sum is over all particles in a jet. The transverse momentum p_t and the pseudorapidity η are calculated with respect to the jet axis. All ten input variables were scaled to give values in the region between zero and one since this simplifies the learning procedure of the network. A transfer function of the form $g(x) = 1/(1 + exp(-2x))$ was used in all nodes and the summed squared error in the network output provided a quality measure of the performance of the network. A training sample of 3000 quark jets and 3000 gluon jets was generated with our complete Monte Carlo chain. The learning rate, which defines the size of the corrections of the weights each time they are adjusted, had an initial value of

0.05 and was set to decay during the learning phase to allow the net to settle in a stable state. When the complete training sample had been presented to the network 200 times the performance of the network was evaluated by a new test sample containing 2000 quark and gluon jets which were correctly identified in 73% of the cases, see Fig. 7c. Correctly identified means that the network gave an output value above 0.5 for a quark jet and a value below 0.5 for a gluon jet.

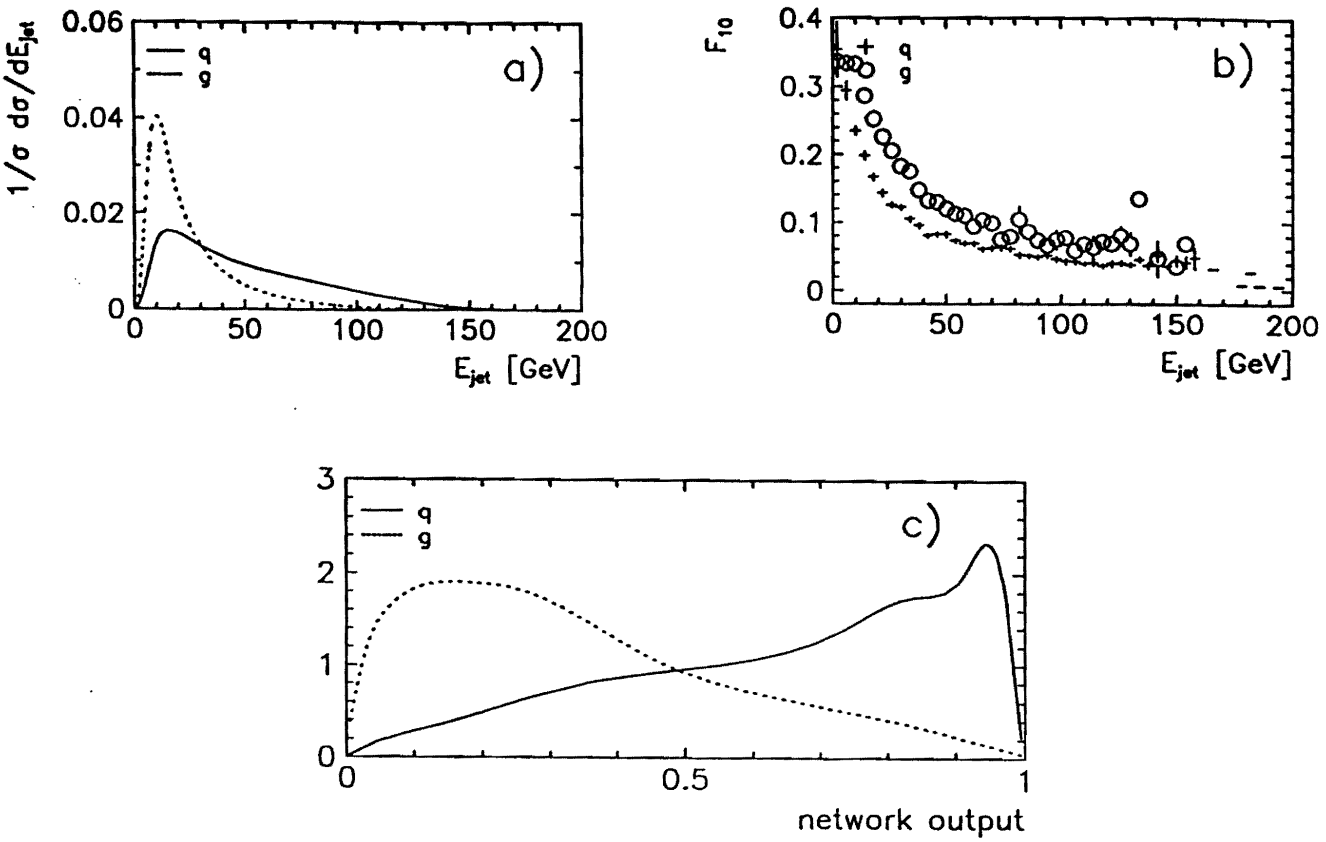

Figure 7: *(a) The energy of quark and gluon jets and (b) an example of a Fodor moment used as input to the neural network. (c) The network output classification of quark and gluon jets.*

Taking advantage of the fact that QCD Compton events must contain exactly one jet of each kind, we required one output value larger than 0.5 and one value smaller than 0.5 for each event. This requirement was fulfilled in 67% of the events for which 86% of the jets were correctly assigned. (In principle, the effect of the remaining missidentification on the final asymmetry results can be corrected for.) It should be pointed out however, that the condition for a succesfull use of the neural network method, based on supervised learning, is that the training sample presented to it has been generated according to a Monte Carlo model which gives a reasonable description of reality. The sensitivity of the network to different models is one way of testing the reliability of the network result. This has not been checked in our particular case, but previous studies of quark and gluon jet separation have indicated that the model dependence is fairly weak [17].

4 Results and conclusions

The final distributions in azimuthal angle for our quark and gluon jets (with $p_\perp \geq 4$ GeV) are given in Fig. 8. After detector simulation a clear asymmetry can still be observed. Close to $\Phi = 0$ there are some discrepancies between the asymmetries after reconstruction and the asymmetries at the generated parton level. These discrepancies may occur if the cuts applied introduce a bias in Φ or if the quality of the reconstruction and identification of jets is correlated with their Φ-angle. Such effects can arise due to the transverse boost between the hadronic cms and the lab system, since a jet with $\vec{p}_\perp$ opposite (parallel) to this boost may loose (gain) $p_\perp$ and therefore be more difficult (easy) to reconstruct properly in the lab system. In particular, small $p_\perp$ jets in the lab system are more likely to be (partly) lost in the beam pipe.

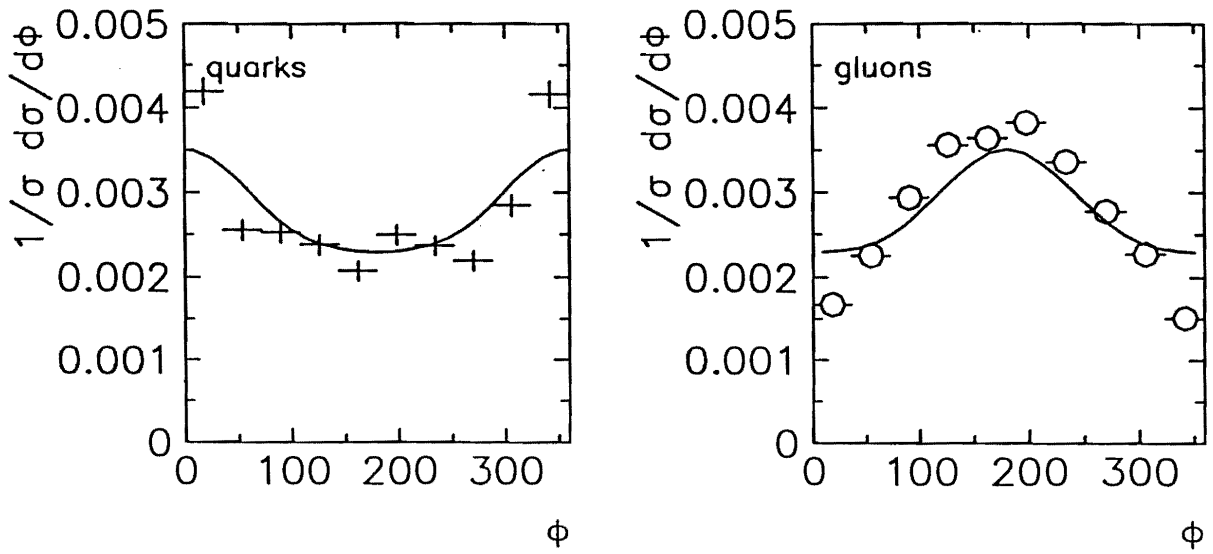

Figure 8: *The reconstructed azimuthal angle distribution for quark and gluon jets (data points) compared to the original parton level distribution (curves). The jets have passed through detector simulation and the sample corresponds to an integrated luminosity of 100 pb^{-1}.*

Fig. 8 is based on a QCD Compton sample with no background. We have found that the fusion process, which should yield the dominating background to our two-jet sample, is about a factor four lower in cross-section and should therefore not influence the results to a large extent. This background will, however, be further reduced by the jet identification which should rarely classify $\gamma g \rightarrow q\bar{q}$ events as having a quark and a gluon jet.

Finally, we would like to mention that the asymmetry in the fusion process can be measured as well. An identification of the quark and antiquark jet is not neccessary, since their distributions in azimuthal angle are identical due to the crossing symmetry of the matrix element, and they can therefore be added together. The background, which in this case is the QCD Compton process, would then give a flat contribution (when quark and gluon jets are added without jet identification) and hence it would not disturb the wanted asymmetry.

References

[1] M. Bengtsson, G. Ingelman, T. Sjöstrand, in Proc. HERA workshop, Hamburg 1987, DESY Hamburg 1988, vol 1, p. 149
M. Bengtsson, G. Ingelman, B. Naroska, *ibid* vol 1, p.281

[2] H. Georgi, H.D. Politzer, Phys. Rev. Lett. 40 (1978) 3
G. Köpp, R. Maciejko, P.M. Zerwas, Nucl. Phys. B144 (1978) 123
A. Mendez, A. Raychaudhuri, V.J. Stenger, Nucl.Phys. B148 (1979) 499

[3] R.N. Cahn, Phys. Lett. 78B (1978) 269

[4] A. König, P. Kroll, Z. Physik C16 (1982) 89

[5] M. Arneodo et al., EMC collaboration, Z. Phys. C34 (1987) 277
A. Mukherjee et al., Phys. Rev. Lett. 60 (1988) 991

[6] J. Chay, S.D. Ellis, W.J. Stirling, Phys. Rev. D45 (1992) 46

[7] G. Ingelman, G.A. Schuler, AROMA 1.2, unpublished program manual
G. Ingelman, G.A. Schuler, Zeitschrift für Physik C40 (1988) 299

[8] G. Ingelman, LEPTO version 5.2, unpublished program manual

[9] B. Andersson, G. Gustafson, G. Ingelman, T. Sjöstrand, Phys. Rep. 97 (1983) 31

[10] T. Sjöstrand, JETSET 6.3, Comp.Phys.Comm. 39 (1986) 347, *ibid* 43 (1987) 367

[11] R. Nisius, P. Schleper et. al., 'A Guide to H1PSI', H1 internal note

[12] H. Albrecht, M. Erdmann, P Schleper, 'PHAN, a physics analysis program for H1'

[13] P. Kooijman, HERA workshop 1991, these proceedings

[14] C. Peterson, T. Rögnvaldsson, Lund preprint LUTP 91-23 to appear in proc. CERN school of computing 1991

[15] L. Lönnblad, C. Peterson and T. Rögnvaldsson, Lund prepint LUTP 91-18, to appear in Comp. Phys. Comm.

[16] Z. Fodor, Phys. Rev. D41, 1726 (1990)

[17] L. Lönnblad, C. Peterson and T. Rögnvaldsson, Nucl. Phys. B349 (1991) 675